A Critical Evaluation of Structural Analysis Tools used for the Design of Large Composite Wind Turbine Rotor Blades under Ultimate and Cycle Loading

Lekou, D.J.; Bacharoudis, K. C.; Farinas, A. B. ; Branner, Kim; Berring, Peter; Croce, A.; Philippidis, T.P.; de Winkel, G. D.

Published in:
Proceedings of the 20th International Conference on Composite Materials

Publication date:
2015

Document Version
Publisher's PDF, also known as Version of record

A CRITICAL EVALUATION OF STRUCTURAL ANALYSIS TOOLS USED FOR THE DESIGN OF LARGE COMPOSITE WIND TURBINE ROTOR BLADES UNDER ULTIMATE AND CYCLE LOADING

D. J. Lekou[1], K. C. Bacharoudis[1], A. B. Farinas[2], K. Branner[3], P. Berring[3], A. Croce[4], T. P. Philippidis[5] and G. D. de Winkel[6]

[1]Centre for Renewable Energy Sources & Saving (CRES)
19th km Marathonos Avenue, GR 19009 Pikermi, Greece
Email: dlekou@cres.gr, web page: http://www.cres.gr

[2]National Renewable Energy Center (CENER)
Ciudad de la Innovación, nº 7, 31621 Sarriguren (Navarra), Spain
Email: afarinas@cener.com, web page: http://www.cener.com

[3]Wind Energy Dept., Technical University of Denmark (DTU)
DTU Risø Campus, Frederiksborgvej 399, DK-4000 Roskilde, Denmark
Email: kibr@dtu.dk, web page: http://www.dtu.dk

[4]Politecnico di Milano (POLIMI)
Piazza Leonardo da Vinci 32, 20133 Milano, Italy
Email: alessandro.croce@polimi.it, web page: http://www.polimi.it

[5]University of Patras (UPAT)
P.O. Box 1401, Panepistimioupolis, GR26504 Rio, Greece
Email: philippidis@mech.upatras.gr, web page: http://www.core.mech.upatras.gr/

[6]Knowledge Centre Wind turbine Materials and Constructions (WMC)
Kluisgat 5, 1771 MV Wieringerwerf, the Netherlands
Email: G.D.deWinkel@wmc.eu, web page: http://www.wmc.eu/

Keywords: Wind Energy, Rotor Blades, Strength, Stiffness

ABSTRACT

Rotor blades for 10-20MW wind turbines may exceed 120m. To meet the demanding requirements of the blade design, structural analysis tools have been developed individually and combined with commercial available ones by blade designers. Due to the various available codes, understanding and estimating the uncertainty introduced in the design calculations by using these tools is needed to allow assessment of the effectiveness of any future design modification. For quantifying the introduced uncertainty a reference base was established within INNWIND.EU in which the several structural analysis concepts are evaluated. This paper shows the major findings of the comparative work performed by six organizations (universities and research institutes) participating in the benchmark exercise. The case concerns a 90m Glass/Epoxy blade of a horizontal axis 10MW wind turbine. The detailed blade geometry, the material properties of the constitutive layers and the aero-elastic loads formed the base by which global and local blade stiffness and strength are evaluated and compared. Static, modal, buckling and fatigue analysis of the blade were performed by each partner using their own tools; fully in-house developed or combined with commercially available ones, with its specific structural analysis approach (thin wall theory and finite element models using beam, shell or solid elements) and their preferable analysis type (linear or geometrical non-linear). Along with sectional mass and stiffness properties, the outcome is compared in terms of displacements, stresses, strains and failure indices at the ply level of the blade structure, eigen-frequencies and eigen-modes, critical buckling loads and Palmgren-Miner damage indices due to cycle loading. Results indicate that differences between estimations range from 0.5% to even 40%, depending on the property compared. Modelling details, e.g. load application on the numerical models and assumptions, e.g. type of analysis, lead to these differences. The paper covers these subjects, presenting the modelling uncertainty derived.

1 INTRODUCTION

The Wind Energy community faces the great challenge to successfully establish cost-effective designs for even larger wind turbines (WTs) with output capacity of 10-20 MW. For these machines, the rotor blades may exceed the length of 120m. To assure safe and affordable design of these huge composite material structures, several innovations should be devised and adopted in current practice. In order to meet the demanding requirements of the structural design of the rotor blade, structural analysis tools have been developed individually and combined with commercial available ones by the blade designers. Yet, due to the various available codes, it is quite difficult to assess the effectiveness of any future design modification without first understanding and estimating the uncertainty introduced in the design calculations by using these tools. Thus, a crucial step, before any new idea comes up, comprises the establishment of a reference base in which the several structural analysis concepts will have been evaluated quantifying the introduced uncertainty.

Actions in this direction have been carried out in the frame of the EC co-funded INNWIND.EU research project [1]. This paper shows the major findings of the comparative work performed by six organizations (universities and research institutes) participating in this benchmark exercise. The case concerns a 90m Glass/Epoxy blade of a horizontal axis 10 MW wind turbine [2]. The detailed blade structure along with the material properties of the constitutive layers and the aero-elastic loads formed the base by which global and local blade stiffness and strength were evaluated and compared. Static, modal, buckling and fatigue analysis of the reference blade were performed. Along with the sectional mass and stiffness properties, the outcome was compared in terms of displacements, stresses, strains and failure indices at the ply level of the blade structure, eigen-frequencies and eigen-modes, critical buckling loads and Palmgren-Miner damage indices due to cycle loading. Results were derived by each partner using their own tools fully in-house developed or combined with commercially available ones, with its specific structural analysis approach (thin wall theory and finite element (FE) models using beam, shell or solid elements) and their preferable analysis type (linear or geometrical non-linear).

Results of this comparative research work are presented focusing on strength and aspects where validation of analysis tools with experimental data (following full-scale blade testing standard) is difficult. Depending on the property, differences between results range from 0.5% to even 40%. Modelling details, e.g. load application on the FE models and assumptions, e.g. type of analysis, lead to these differences. The paper covers these subjects, indicating the modelling uncertainty derived.

2 BASELINE OF THE BENCHMARK

Detailed description of the blade geometry and structural configuration was provided by DTU to all partners for this benchmark. For the structural benchmark only the straight version of the DTU 10MW reference blade [2] is used. That is the models of the blade run by the participants did not include pre-bending. The blade model starts at z_0 = 2.8m and ends at z_L = 89.166m. Details between the blade root and the rotor centre were ignored in this benchmark. The detailed external geometry of the blade, i.e. the coordinates of sections defined along the blade length, was provided by DTU. The internal structure of the blade was also provided at the same level of detail. This included following information:

- Material distribution (position of each lamination sequence on the section and along the blade)
- Lamination sequences (on a layer by layer basis the thickness of the layer, the orientation of the fibres and the material type of each composite layer in the stacking sequence)
- Material properties (mechanical properties for each anisotropic composite material layer)

The above information was combined with specific locations for output reporting, as well as with specific of loading that was used in each analysis. Detailed comparison was performed at 5 reference sections along the blade; the root section (r/R = 3%), a section near the maximum chord (r/R = 30%) and three sections at r/R equal to 43%, 60% and 80%, respectively. The key points (KP) and the segments where the deflection, stress and strain values as well as damage index (fatigue) values are compared for each of the reference sections are illustrated in Figure 1. KP1 is located on the pressure side Trailing Edge segment and KP5, KP9 and KP12 are consequently numbered counter-clockwise around the section. KP5 is connected to elements (and therefore lamination sequences) in the trailing

panel (left on the figure), the spar cap on the pressure side of the section (right on the figure) and the shear web towards the trailing edge (up on the figure). KP9 is at the nose of the leading edge, while KP12 is a point on the spar cap of the suction side of the blade.

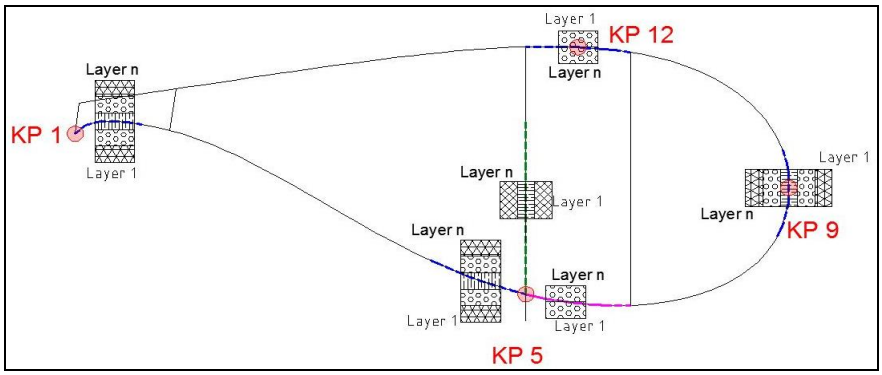

Figure 1: Key point numbering definition and lamination sequence direction

For the strength estimations (static and buckling analysis) to compare methods and criteria used, disregarding failure criteria employed, simulations are run in two steps; First step involves running simulation using the reference load as given and checking whether failure is predicted or not. Failure was defined by each partner, following approaches acceptable in a blade certification procedure such as [3]. In the second step, the load is modified (by multiplying it with a coefficient) until load with the opposite prediction is obtained. For example, if, when applying the reference load (extreme case evaluation), no failure is predicted for the whole blade then, the load is multiplied to reach the load where failure is first predicted. The coefficient used for the load increase is then reported. Otherwise, if failure is predicted under the reference load, then the load is reduced until there is no prediction of failure.

2.1 Loading conditions

The reference load case selected for the benchmark on blade structural models under static and buckling analysis is representing an extreme load case formed by selecting for each reference section along the blade the aero-elastic simulation output corresponding to the maximum resultant bending moment provided by DTU in [2]. The data provided to the partners participating in the comparison exercise presented sectional stress resultants (forces and moments) on each section.

The proposed load case does not describe simultaneous applied loads across all sections and it does not cover all load cases that the blade should sustain. Therefore, this might result to non-conservative or conservative results regarding the blade strength output. However, this reference load case was considered to be effective for the purposes of the benchmark.

In order to reduce the variability in simulation results stemming from the translation of the sectional stress resultants to external loads, especially in 3-dimensional finite element models a simple load case was also provided for results comparison within the benchmark. In this, the external forces that should be applied (e.g. in a FEM model) were provided to the participants, specifying magnitude and position along the blade, to form a "simple" load case to be used in the benchmark. These external forces have been estimated using the reference load case, following the procedure used in blade testing to define the loads that should be applied on the blade.

The reference load case selected for the benchmark on variable load blade structural models comprises normal operational cases and parked (standstill or idling) cases covering the whole range of potential wind speeds, under the assumptions explained in this section. The time series are provided by POLIMI as results of POLIMI's aero-elastic analysis of the reference wind turbine. Aero-elastic simulations were run following the normal turbulence model for the wind inflow (NTM) corresponding to design load case DLC11 and only one seed, which for the benchmark case with specified load conditions does not influence the comparison of results. The parked load cases correspond to DLC64. The simulations by POLIMI were computed with the INNWIND.EU baseline blade [2] using the same control parameters but without pre-bending. The latter was selected to match

the structural benchmark on extreme loading, which is also performed on the straight blade. Time series of sectional stress resultants (forces and moments) on the reference sections along the blade were provided to the participants in the comparison exercise.

For the definition of the load sequence representative of the complete life of the blade on the wind turbine following parameters have been assumed: i) the operational life of the blade is 25 years, ii) the average wind speed at the site is equal to 10m/s and iii) the wind speed follows a Weibull distribution with k parameter equal to 2 (i.e. corresponding to Rayleigh distribution).

The number of occurrences of the each load case with a specific 10-min average wind speed was provided to the partners in the benchmark. It is recognized that the proposed load sequence does not comply with the requirements of the design standards relevant to the number of simulations and number of load cases included in the simulation. But, this does not affect the benchmark results relevant to the fatigue analysis tools of the partners.

2.2 Structural analysis tools used by the partners

Six organizations participated in the benchmark on structural analysis tools for wind turbine blades. The results provided by each participant in the benchmark were estimated by different tools by the partners, as shown in Table 1. All partners used commercial finite element software indicated by FEM in Table 1 to provide part (or all) of the data. In Table 1, by 2D FEM, FE models using beam elements are implied, 3D FEM implies the use of shell elements and SOFEM implies use of solid elements. The FE software used by the partners was for CRES NISA II (EMRC). For CENER, MSC.Patran was used for modelling in combination with MSC.Nastran solver. DTU also used MSC.Patran for modelling in combination with the in-house tool BECAS [7], but MSC.Marc was used as the solver. MSC.Marc was also used as a solver for the buckling analysis using commercial FE software by WMC. POLIMI used MSC Nastran 2011 for data extracted by FE models, while UPAT used ANSYS. In house developed tools which were used for extraction of data by the partners are explicitly mentioned in the following table (Table 1). As indicated in the table, some partners used more than one model for a specific analysis type.

Results for	CRES	CENER	DTU	PoliMi	UPAT	WMC
Global blade properties	3D FEM	BASSF [4]+ 3D FEM	SOFEM	3D FEM	3D FEM	FOCUS6 [10]
Natural frequencies	3D FEM	2D FEM+ 3D FEM	SOFEM	3D FEM	3D FEM	FOCUS6
Buckling analysis	3D FEM	---	SOFEM	3D FEM	3D FEM	3D FEM+ FOCUS6
Section properties	THIN [5][4],[6]	BASSF	BECAS	ANBA [8]	PROBUST [9]	FOCUS6
Displacements	3D FEM	2D FEM+ 3D FEM	SOFEM	3D FEM	3D FEM	FOCUS6
Strength analysis	3D FEM + THIN	BASSF+ 3D FEM	SOFEM	3D FEM	3D FEM + PROBUST	FOCUS6
Strains	3D FEM	BASSF+ 3D FEM	SOFEM	3D FEM	3D FEM	FOCUS6
Stresses	3D FEM + THIN	BASSF+ 3D FEM	SOFEM	3D FEM	3D FEM	FOCUS6
Rainflow Counting	[11]	---	---	---	[12]	[13]
Stresses (Fatigue)	THIN	---	---	3D FEM	PROBUST	FOCUS 6

Table 1: Tools used by partners

In the benchmark of fatigue tools 4 organizations participated. Concerning the cycle counting method, all partners used the well-known rainflow counting technique implementing various algorithms proposed in the literature, as shown in Table 1. Despite the slight differences, all the employed algorithms have in common the searching procedure, a four point searching algorithm that is used to identify the range-pairs and “residu” for every peak/trough sequence. For the calculation of the

linear damage index, stresses/strains at the ply level of the blade structure must be computed at some stage of the calculation procedure. Tools used for these calculations are summarized in Table 1.

3 RESULTS

While a comparison regarding the sectional properties of a blade, e.g. bending stiffness, mass inertia and shear centre as obtained by several available tools has been reported in the past, [14], it is the first time that the comparison extends to modal analysis, as well as strength results. In [14] large differences for the cross-section properties were reported among the compared tools. Differences reaching even 100%. Yet, in the present work, the differences were found quite small.

Specifically, as an initial check to assure correctness of input data interpretation the total mass and centre of gravity for the whole blade, was compared for all models. A coefficient of variation of less than 1% is obtained for the total mass and of 1% for the centre of gravity with respect to the blade length. The results for the centre of gravity relative to the flap direction show a standard deviation of 0.002m (2mm) and in the edge direction 0.03m (30mm) on a section having a chord of about 6m. Taking into account the different modelling approaches employed the results are in very good agreement.

Mass and stiffness sectional properties were requested to compare data that are provided for performing an aero-elastic analysis upon structural design information of the blade. The data should be provided with respect to a commonly agreed global coordinate system, although each participant uses its own reference system. This constraint revealed larger deviations for properties that are affected by the selection of reference points and coordinate systems, such as the coordinates of the mass and/or elastic centre on the section and the properties incorporating the 2nd moment of inertias.

The coefficient of variation for the linear mass ranges from 1% to 2.1%, while the worst coefficient of variation for the 5 sections along the blade of the mass moment of inertia (ρI) in the flap direction is 6.6% in the edge direction is 12.4% and the cross term is 14.5%. As already noted the dispersion of the mass centre coordinates and the coupling term of the mass moment of inertia, which depend on the coordinate system and are small values, is larger. The standard deviation of the mass centre in the edge (chord) direction reaches 0.089m for reference section 2, while the standard deviation on the same section in the flap (thickness) direction reaches 0.0154m.

The location of the mass, elastic and shear centre is shown in Figure 2 for reference section 2 (r/R = 30%) with respect to the section's dimensions. The small dispersion in prediction of the location of the mass, elastic and shear centres is evident in this figure, despite the absolute number of coefficient of variation of even 700%.

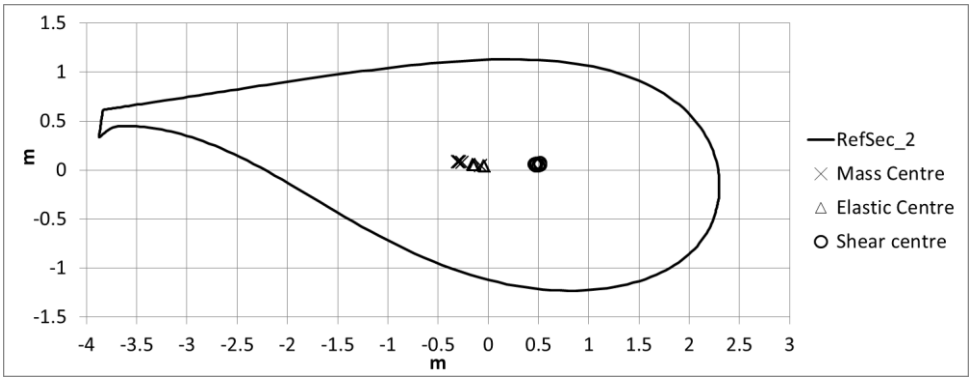

Figure 2: Location of mass, elastic and shear centre on RefSec_2 (r/R = 30%)

Regarding the location of the elastic centre on the section, the standard deviation of the reported values is less than 0.05m in the x direction (chord) and less than 0.008m in the y direction (thickness). One partner had a strong deviation from the others in the x-location. For the shear centre, the dispersion of results is a little larger than that of the elastic centre, but comparable. The standard deviation in this case is less than 0.03m (for the x direction).

Relevant to the rest of the stiffness properties from the 5 reference sections along the length, the axial stiffness has a coefficient of variation ranging from 0.7% to 1.8%, the worst coefficient of variation of the bending stiffness (EI) in the flap and edge direction is 6.4% (on different section nevertheless), while for the cross-term it is 9.2% and the torsional stiffness (GJ) has a maximum coefficient of variation equal to 13%. Only three participants reported on shear stiffness. The values differ for the root section, but for the other sections their difference is close to the difference of the torsional stiffness.

3.1 Modal analysis results

The results for the modal analysis are collectively presented in Table 2. Results are in very good agreement up to and including the 5th mode of vibration. For most of the partners modes 1, 3 and 5 correspond to the first three bending natural frequencies in the flap direction, whereas modes 2, 4 refer to the first two bending natural frequencies in the edge direction of the structure. Actually, results of mode shapes reveal the existence of a small coupling between the flapwise and the edgewise mode-shapes of the blade. With the exception of one partner, the 6th mode identified corresponds to a torsional mode. Partner A identified the torsional mode under the 7th mode, shown in the table.

Mode	A	B	C	D	E	F	G	Average	StDev	CoV (%)
1	0.64	0.62	0.61	0.61	0.61	0.61	0.62	0.62	0.011	1.8
2	0.96	0.99	0.97	0.95	0.91	0.95	0.97	0.96	0.024	2.5
3	1.85	1.81	1.75	1.74	1.74	1.75	1.80	1.78	0.042	2.3
4	2.86	3.00	2.88	2.87	2.77	2.83	2.98	2.88	0.080	2.8
5	3.76	3.77	3.56	3.52	3.55	3.57	3.77	3.65	0.117	3.2
6	5.82	6.23	5.61	5.53	5.70	5.55	6.17	5.80	0.291	5.0
7	6.01									

Table 2: Natural frequencies of the blade (all frequencies in Hz)

For the first mode of vibration (flap direction) the coefficient of variation among the partners' results is 1.8%, while for the second mode of vibration (in the edge direction) the coefficient of variation is 2.5%. The coefficient of variation for the modes 3-5 varies between 2.3% and 3.2%. The results for the 6th mode of vibration lead to a coefficient of variation of 5%. A similar coefficient of variation (5.6%) and a comparable average value (5.815Hz) is obtained if the torsional modes of vibration reported by partnres are treated disregarding the mode number. It is evident that the largest uncertainty is identified for the torsion response of the blade. This is also shown from the deflection analysis presented in the following section.

3.2 Deflection results

Results for the deflection along the blade in the flap direction for the simple and reference load case are shown in Figure 3. For the simple case one partner performed a geometrically non-linear analysis and for comparison purposes reported also the results at 5% load scaled to full load. Both curves along the blade are shown in the left graph of Figure 3. For the two load cases Table 3 shows the average values of the displacement along the blade length, as well as the coefficient of variation observed in the flap and edge direction. Results for the simple load case are in better agreement than for the reference load case, as expected, because of the constraint posed on modelling the applied load. The non-linear solution falls within the estimation of the other (linear) predictions. The only difference being that the displacement in the z-direction (along the blade) for the non-linear solution approaches the magnitude of that in the x-direction (edge direction).

The data provided by the partners allow for a simplified estimation of torsion along the blade length. Since the displacements are provided for 4 key points on the section, which more or less form a rhombus, the difference between the rhombus's diagonals before and after loading can be used as a measure of torsion on the sections. Considering the mean value between the two results (torsion between trailing edge and nose at leading edge, as well as torsion between cap of suction and suction

side) from each partner the torsion for the reference case is shown in Figure 4. Two groups are clearly formed and these are connected with the fact that partners predicting larger torsion values are using links in modelling the applied forces, while those with the smaller results directly apply loads on the shell structure.

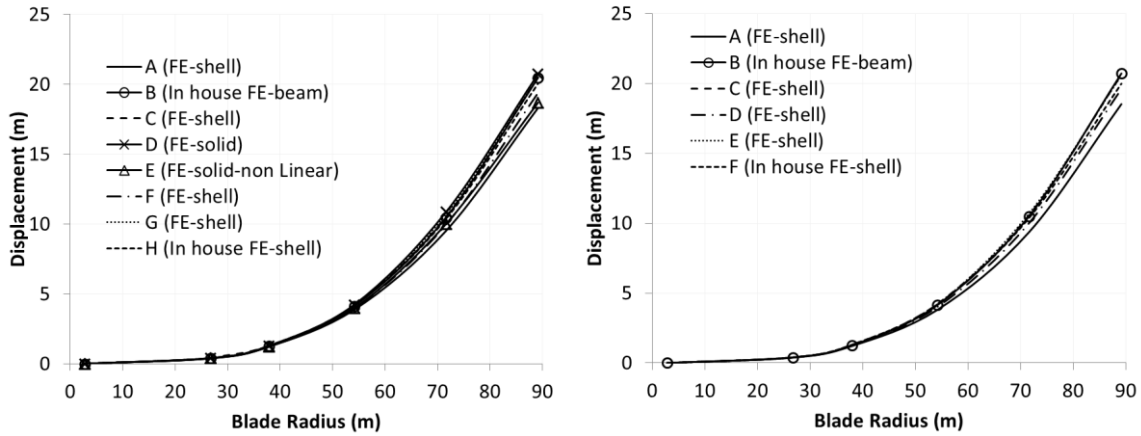

Figure 3: Displacement in the flap direction for the simple (left) and the reference load case (right)

	Simple load case				Reference load case			
	Flap		Edge		Flap		Edge	
Position (m)	Average (m)	CoV (%)	Average (m)	CoV (%)	Average (m)	CoV (%)	Average (m)	CoV (%)
2.800	0	--	0	--	0	--	0	--
26.694	0.394	2.2	0.188	9.1	0.397	1.9	0.187	12.8
37.907	1.259	2.4	0.483	5.9	1.266	2.9	0.467	12.0
54.149	4.084	3.2	1.171	5.9	4.085	3.9	1.123	11.8
71.592	10.283	4.3	2.177	7.1	10.245	4.8	2.062	13.0
89.166	19.828	4.7	3.264	7.7	20.014	4.2	3.053	14.6

Table 3: Deflection average and coefficient of variation along the blade in flap and edge direction for the simple load case (left) and the reference case (right)

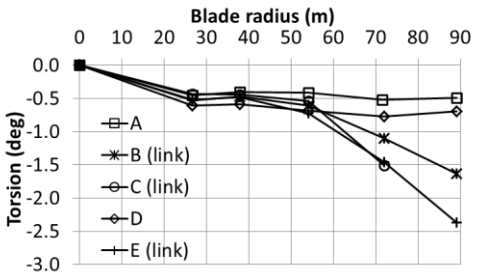

Figure 4: Simplified torsion estimation under reference load case along the blade length

3.3 Buckling results

The dispersion of results of the buckling analysis performed is quite high. Buckling load factor ranges from 1.8 to 3.1. The numerical model of the blade, the analysis followed as well as the modelling of the load on the blade have a crucial effect on the predictions. Even the buckling location was found different with other partners locating the mode shape in the root area (on the suction side spar cap) of the blade and others around 75% of the rotor radius (at the trailing edge region). A detailed analysis performed by one partner looking into higher buckling modes revealed that the first five eigen-modes are quite close together (in the range 1.9 to 2.0, corresponding to a difference of 5%

over the original result), while there is also a mode shape change in the 5th mode, moving the location of the buckling from the root area of the blade to the outboard part. This observation justifies the differences observed in buckling location, since slight modifications on the applied load pattern can easily lead to an adjacent mode shape with nearly the same load factor.

Gross stiffness does not seem to play an important role, since those partners that have estimated lower deflections under the static analysis do not predict higher buckling load factors. The difference are more so coming from local modelling details. The effect of distributing the applied load on all nodes of the section or on nodes of the spar caps only was investigated by another partner, revealing a difference of 4% between results.The effect of using the simple load case or the reference one, was studied by a third partner showing a difference in buckling prediction of 7%. The coefficient of variation between partners results on the reference load case was estimated to 23% with the average buckling load factor being 2.2.

3.4 Extreme load carrying capacity results

The choice of failure criterion was open to partners for the case of the extreme load carrying capacity, limited only by recommendations from certification bodies (e.g. [3],[15]). First ply failure was considered and progressive damage was not taken into account. Several partners used the Tsai-Wu failure criterion, with the Tsai-Hahn expression for the coupling term. One partner provided data with several formulations of the Tsai-Wu criterion including the Tsai-Hahn the Hoffman and the Hill failure criterion, in addition to the maximum strain and the Puck criterion checking fibre and inter fibre failure. The maximum strain criterion and the Puck failure criteria were used by two partners, while another partner used also the the maximum stress criterion.

Agreement was achieved for the location of the critical failure area among the partners. Except for one case, all participants estimated the critical area to be in the suction side of the blade, close to the maximum chord section and towards the leading edge. But, the estimation of the load criticality, i.e. the ratio of the load where failure is predicted against the reference load used in the benchmark is quite different depending on the numerical model, on the failure criterion used, but also on the modelling of the applied load on the blade.

Results indicate that the coefficient of variation of the partner estimating failure by 4 different failure criteria but using the same model ranges from 5 to 10%. Lower difference is shown when the load is distributed only on the spar cap nodes, while if the applied load is distributed on all nodes around the section then the scatter of estimations increases. The effect of the failure criteria on the predictions has been studied earlier, as e.g. [16] and differences are within the expected range.

The coefficient of variation from results of partners using the same failure criterion, i.e. Tsai-Hahn formulation, is found 20%. The different models used, as well as differences in modelling of the applied load lead to this scatter. Distribution of the load on more nodes around the section, has a benign effect on the prediction of failure, which could reach even prediction of failure at 20% higher load. There are also indications that a similar benign effect is observed when sectional analysis tools are employed, in which case the loading is considered through residual loads of the section, rather than external applied loads.

3.5 Fatigue results

For fatigue strength, the failure model employed by all partners in the benchmark is based on GL's [3] approach. Following the GL design guideline [3] the constant life diagram (Goodman diagram) in absence of experimental data is described per:

$$N = \left[\frac{R_{k,t} + |R_{k,c}| - |2\gamma_{MA} S_{k,M} - R_{k,t} + |R_{k,c}||}{2(\gamma_{MB} / C_{1B}) S_{k,A}} \right]^m \quad (1)$$

Where N is the allowable number of cycles, $S_{k,M}$ and $S_{k,A}$ denote the mean value and the amplitude, respectively of the characteristic actions (loads), m equals 10 for Glass/epoxy composites, $R_{k,t}$ and $R_{k,c}$ are the characteristic short-term structural member resistance for tension and compression, γ_{MA}, the material safety factor for extreme analysis, was taken equal to 2.205 for the benchmark, C_{1B} is $N^{1/m}$

and γ_{MB} is the material safety factor for fatigue analysis. The above expression can be used both in strain format as well in stresses format.

To identify differences that might influence the fatigue strength results comparisons were performed also in the rainflow counting algorithms and strategies of each partner. The accumulated number of full cycles against the range showed small differences as shown in Figure 5 (left), although partners used different discretization on the cycle range (20, 50, 64 and 128 bins), as well as different handling of residues. Comparison of rainflow counting against the range have been also performed in the past.

In the fatigue analysis of composite materials and following the design guidelines for wind turbine blades (e.g. GL), except for the range, the mean value also plays a vital role in the estimation of the fatigue life of a structural component. Therefore, to shed more light in the interpretation of the results regarding damage estimation, a comparison also relevant to the mean value reported should be performed. The best way to do that would be a contour plot, with x and y axis the mean and range value of the bin and the contour referring to the number of cycles in the bin. Yet, due to the differences in the bin definition by each participant it is quite difficult to compare the graphs visually. Therefore, a new type of graph was presented: Plots of the mean value against the accumulated number of full cycle are depicted in Figure 5 (right) for the Mx moment stress resultants at the RefSec_2 (r/R=30%). The horizontal axis (x-axis) of the graph is in logarithmic scale, again. But, note is to be taken that the following curves cannot be interpreted as the traditional cumulative load curves (shown left). While the effect of the range magnitude is clear on the fatigue damage of the material, the effect of mean can be interpreted only if combined with the range. Therefore, in case of the cumulative number of cycles ploted against the mean value the graph should be interpreted as: the bending moment stress resultant has a cumulative number of cycles (read from x-axis) which have mean below the mean value (read from y-axis). As for the range, the discretization of the mean value in bins was different between the partners; 32, 50 and 64 bins were used.

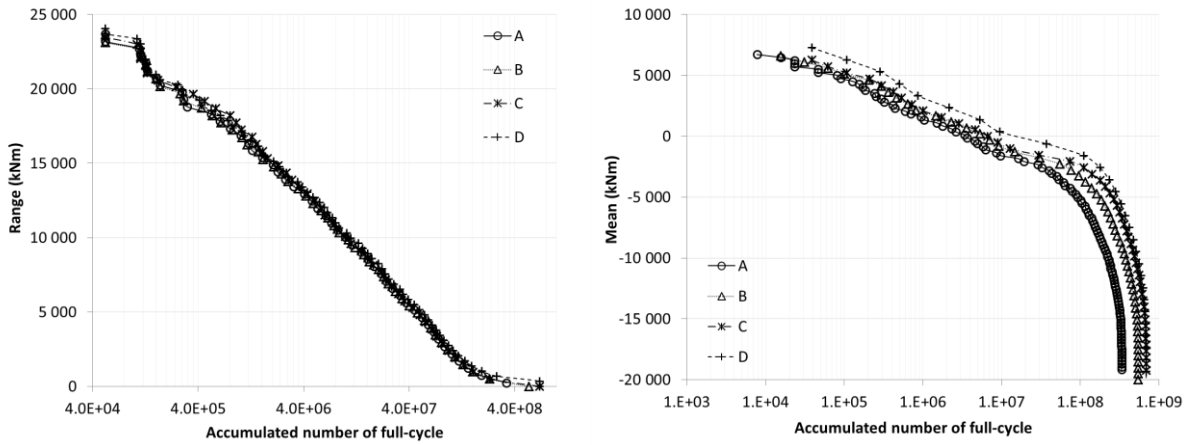

Figure 5: Accumulated number of full-cycles for the bending moment stress resultant in the flap direction against range (left) and mean value for RefSec_2 (r/R=30%)

Larger deviations exist between the partners in the case of the mean values, than in the case for the range values. Again, these differences noticed could be attributed to small variations in handling of residues and threshold used (if applicable) in counting cycles.

For comparing the damage index results, the fatigue stress factor (FSF) is used, whereby if the applied stresses are multiplied with this factor you obtain a damage index of 1 [17]. This quantity scales like $D^{(-1/m)}$, where D is the Palmgren-Miner damage index and m equals 10 for Glass/epoxy composites as per eq.(1). In Figure 6 the minimum fatigue stress factor over all layers in the lamination sequence is presented for two sections (r/R equal to 30% and 60%) at 6 key points (see Figure 1) around each reference section.

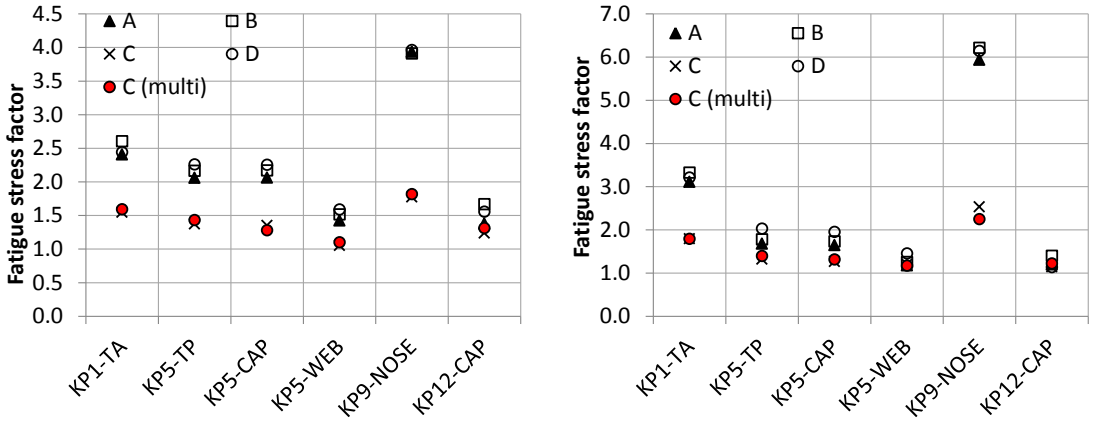

Figure 6: Fatigue stress factor in RefSec_2 (r/R=30%) left and RefSec_4 (r/R=60%) right

The diversity on the fatigue stress factor and in turn also the damage index values as calculated by each partner is evident, although the failure criterion is common to all. The largest coefficient of variation among the fatigue stress factors estimated reaches 34% at the leading edge nose of the outboard section (at r/R=60%). This is due to the differences of the stress analysis tools and the rainflow counting algorithms used by the partners. For example, also when comparing stress and strain output under static load it was noticed that some tools underestimated the stresses developed at specific key points, due to specific assumptions in the model. These differences are now mixed with the dissimilarities of the rainflow counting algorithms and strategies followed by each partner (discussed earlier). Analysis of the effect of the stiffness of the section on the fatigue results was performed.

Further to that, one would expect that taking into consideration the multi-axial state of stress, of the material (as per [18], [19]) would result in an increased damage index than considering only the longitudinal stress. Yet, as shown by results from one partner running both cases, indicated as case C and C (multi) in the graphs, this is not always the case. In fact for some specific key points the results (between uniaxial and multi-axial criterion) are reversed with the uniaxial criterion giving a more conservative output. This is also seen in Figure 6 presented above, e.g. on KP5 for RefSec_2, but also on the values directly reported by the partner.

From the study performed it was shown that differences in fatigue analysis results can occur because of differences in: a) the blade model, b) the calculation method of the stresses, c) rainflow counting method used (including parameters such as the bin size) and d) the calculation of the damage from a pair of stress mean and amplitude. But, differences in the rainflow counting results found due to different choices of bin size and threshold the differences in the fatigue index of up to a factor of 6 could not be explained, if differences in stiffness properties used in the calculation are not taken into account. Relatively small differences in the stiffness magnify differences in the damage index because of the slope of 10.

4 CONCLUSIONS

The work performed within the INNWIND.EU project and presented in here sets the baseline for the estimation of model uncertainty. As all partners were provided with the same information regarding the blade external structure, the internal material lay-out and configuration, as well as the loading that should be imposed on the blade it is possible to compare the output and assess the variability of the results. At this stage neither the accuracy nor the correctness of the numerical simulation results can be assessed, since for that purpose comparison against experimental data should be available. Yet, given the capacity of the participants in the benchmark study and their experience in comparing numerical simulation results of wind turbine blades against test data the relevance of the results is evident. Further to that the number of independent results increases the statistical significance of the data.

The results show that the gross properties of the blade (mass and center of gravity) are estimated

with a very low variation between the partners. A little higher was the coefficient of variation for the sectional mass properties (linear mass and mass moment of inertia). Disregarding small inconsistencies observed the coefficient of variation for mass properties of inertia is about 5%, while the standard deviation of the mass center on the section is below 90mm in the edge and 20mm in the flap direction (on section with 6m chord). Similar results are obtained for the sectional elastic properties (axial, bending and torsional stiffness, elastic and shear center). Yet, this exercise revealed the importance of consistently reporting on the coordinate system of reference if data are to be exchanged between partners with different simulation tools. This is especially important for providing blade structural data for performing aero-elastic analysis.

The coefficient of variation for the natural frequencies of the blade was found to be below 3% up to the 5th mode of vibration, i.e. mainly flap and edge modes. A larger coefficient of variation of about 5% was noticed for the torsional eigen-frequency of blade. Regarding the tip deflection of the blade under load, in two different load cases the coefficient of variation was found below 7% for the flap direction and up to 15% for the edge direction. These results include different modelling methods for the load, i.e. whether loads are directly applied on the shell nodes or through links with a reference node, as well as results from geometrically non-linear analysis. The variation noted for the deflections is considerably reduced if the results of two partners are excluded. Specifically, disregarding results of a partner that did not include the third shear web of the reference blade in the model, as well as that, which modelled the mid-plane of the shell elements on the external surface of the blade, the coefficient of variation for the displacement drops to below 3%. The results by non-linear geometric analysis are close to the average of the other partners, possibly indicating that a linear analysis suffices for this case.

The results on the torsion of the blade revealed larger differences. In this case, all differences in modelling affect the results. That is, even when excluding partners with modelling differences in the internal structure of the blade, as per the deflections, the standard deviation of the torsion is 1 degree. The difference in the torsion at the tip of the blade for the linear and the non-linear case is above 1 degree, indicating that the analysis type has an effect on the results for this case. Further to that, the different modelling of the imposed loads, as discussed in the previous section, also affects the results, leading to a difference of about 2 degrees.

Coefficients of variation of strain data reported within the benchmark were below 5% for longitudinal strains (along the blade direction) for positions on the spar caps, but, they were above 15% for positions on the leading edge and close to the trailing edge of blade. Even larger differences were obtained for the shear and transverse strains, irrespective of the position on the blade.

The same large differences were obtained for predictions of strength. Whether buckling, strength under extreme loads or fatigue, the estimations where in some cases double.

Even for buckling predictions, which depend only on the (local) stiffness and the loading, the differences were above 50%. The modelling of loads was found as playing a significant role in these. Probably the differences in local stiffness, as indicated by strain/stress results also play a significant role. Similar for strength predictions under extreme loading, where multiaxial stress was taken into consideration by the participants there were large differences. Less was the difference for strength prediction under fatigue, but in this case the failure criterion was common to all and (mainly) only longitudinal stress was considered.

It becomes therefore, obvious that to reduce the modelling uncertainty obtained through the benchmark presented experimental data are required. Yet, also the experimental data involve uncertainties that might intervene and potential blur the statistical interpretation of the results. These include not only measurement uncertainties, but also the definition of failure under static and cyclic load. To note is that in the present work failure is taken in a first ply failure condition, which during an experiment is difficult to obtain, even with the use of methods such as acoustic emission.

ACKNOWLEDGEMENTS

The research leading to these results has received funding from the European Community's Seventh Framework Programme FP7-ENERGY-2012-1-2STAGE under grant agreement No. 308974 (INNWIND.EU).

REFERENCES

[1] www.innwind.eu

[2] Bak C, Zahle F, Bitsche R, Kim T, Yde A, Henriksen LC, Hansen MH, Blasques JPAA, Gaunaa M, Natarajan A. The DTU 10-MW Reference Wind Turbine. *Danish Wind Power Research 2013, Fredericia, Denmark, May 27 2013*.

[3] Germanischer Lloyd, Guideline for the certification of wind turbines, 2010

[4] Fariñas AB, Nuin I. Nueva versión BASSF (Blade Analysis Stress Strain Failure) v8.x. Software para diseño preliminar de palas eólicas. *Eolus*, **70**, 2014 (in Spanish)

[5] Lekou DJ, Philippidis TP. PRE-and POST_THIN: A Tool for the Probabilistic Design and Analysis of Composite Rotor Blade Strength, *Wind Energy*, **12(7)**, 2009, pp. 676-691

[6] Philippidis TP, Vassilopoulos AP, Katopis KG, Voutsinas SG. THIN/PROBEAM: A software for fatigue design and analysis of composite rotor blades, *Wind Engineering*, **20(5)**, 1996, pp. 349-362

[7] Blasques JP, Bitsche R, Fedorov V, Eder M. Applications of the BEam Cross section Analysis Software (BECAS), *Proceedings of the 26th Nordic Seminar on Computational Mechanics*, Logg A, Mardal KA (Eds.), Oslo, Norway, 2013

[8] Giavotto V, Borri M, Mantegazza P, Ghiringhelli G. Anisotropic beam theory and applications. *Comput. Struct.* **16**, 1983, pp. 403–413

[9] Bacharoudis KC, Philippidis TP. Estimating design reliability of composite rotor blades under ultimate loading, *Wind Energy* **18(5)**, 2015, 783-796

[10] Brood RRH, Numan R, De Ruiter MJ, De Winkel GD. Focus 6 – Integrated modular wind turbine design tool, presented in Sandia Blade Workshop 2010, 2010 http://windpower.sandia.gov/2010BladeWorkshop/PDFs/2-2-E-2-Numan.pdf

[11] Madsen PH, Dekker JWM, Thor SE, McAnulty K, Matthies H, Thresher RW. Recommended practices for wind turbine testing: 3. Fatigue Loads. 2nd ed., International Energy Agency Wind publications, 1990

[12] Downing SD, Socie DF. Simple rainflow counting algorithms. *Int. J. Fatigue*, **4**, 1982, pp. 31-40

[13] Brokate M, Dreßler K, Krejčí P. Rainflow counting and energy dissipation for hysteresis models in elastoplasticity. *Eur. J. Mech. A/Solids*, **15**, 1996, pp. 705-737

[14] Chen H, Yu W, Capellaro M. A critical assessment of computer tools for calculating composite wind turbine blade properties, *Wind Energy*, **13(6)**, 2010, 497-516

[15] DNV-DS-J102, Design and Manufacture of Wind Turbine Blades, Offshore and Onshore Wind Turbines, *Det Norsk Veritas*, 2010

[16] Soden PD, Kaddour AS, Hinton MJ. Recommendations for designers and researchers resulting from the world-wide failure exercise, *Comp. Scie. & Techn.*, **64**, 2004, pp. 589-604

[17] Heijdra JJ, Borst MS, Van Delft DRV. Wind turbine blade structural performance testing, in *Advances in Wind Turbine Blade Design and materials*, Edited by P. Broendsted, R. P. L. Nijssen, Woodhead Publishing Series in Energy No. 47, Woodhead Publishing Limited, pp. 432-445, 2013

[18] Philippidis TP, Vassilopoulos AP. Complex stress state effect on fatigue life of GRP laminates; Part I, experimental, *International Journal of Fatigue*, **24**, 2002, pp. 813-823

[19] Philippidis TP, Vassilopoulos AP. Complex stress state effect on fatigue life of GRP laminates; Part II, theoretical formulation, *International Journal of Fatigue*, **24**, 2002, pp. 825-830